Chapter 7
Optimal Reactive Power Control to Improve Stability of Voltage in Power Systems

Ali Ghasemi Marzbali, Milad Gheydi, Hossein Samadyar, Ruhollah Hoseyni Fashami, Mohammad Eslami and Mohammad Javad Golkar

Abstract The current power systems have works near to the marginal voltage stability due to the market performance as well as their weightier operation loadings along with consideration of environmental constraints of transmission as well as generation capacity enlargement. In other words, at the present time wind power has confirmed to be one of the most efficient and competitive renewable resources and therefore, its use is indeed continually growing. Little wind power infiltration planes are generally contained in the current grid networks in view of that it is passively controlled and operated. On the other hand, this statement is no more suitable for immediately after the wind power energy infiltration commences

A. Ghasemi Marzbali (✉)
Technical Engineering Department, University of Mohaghegh Ardabili, Ardabil, Iran
e-mail: ghasemi.agm@gmail.com

M. Gheydi · H. Samadyar
Young Researchers and Elites club, Science and Research Branch, Islamic Azad University, Tehran, Iran
e-mail: gheydi.m@srbiau.org

H. Samadyar
e-mail: hosseinsamadyar@yahoo.com

R.H. Fashami
Electrical Engineering Department, Damavand Branch, Islamic Azad University, Tehran, Iran
e-mail: rhfashami@gmail.com

M. Eslami
Department of Electrical and Computer Engineering, Nikshahr Branch, Islamic Azad University, Zahedan Branch, Nikshahr, Iran
e-mail: mohammad.eslami@chmail.ir

M.J. Golkar
Department of Electrical and Computer Engineering, Zahedan Branch, Islamic Azad University, Zahedan, Iran
e-mail: javad.golkar.1368@gmail.com

N. Mahdavi Tabatabaei et al. (eds.), *Reactive Power Control in AC Power Systems*, Power Systems, DOI 10.1007/978-3-319-51118-4_7

growing, a broad scope of scientific issues can come out, namely: voltage rise, bi-directional power flow, improved power quality issues as well as distorted voltage stability. The additional improvement of electricity construction from renewable resources in a trustworthy as well as consistent system performance is driving transmission as well as distribution control utilizers to employ novel working models that are not presently extant. A serious subject of the demanding status described in the foregoing is the reactive power managing that involves the planning as well as operation deeds that are asked for to be executed to get better voltage profile as well as stability in the power networks. For this reason, voltage stability is a major issue of current power systems. It signifies the capableness of a power system to keep voltage when the required load is boosted. Researches about this kind of instability fact proceed with its control as well as evaluation. The first one designates if a power system runs in the safe operational area, while the second one will carry out essential control actions if a power system gets close to unsafe operational zone. Diverse approaches put forth in the chapter deal with offline and online purposes. The center of attention of this chapter is the second part; it means control of voltage stability. Three major methods have been utilized for voltage stability which are reactive power management, load shedding and active power re-dispatch. Reactive power management signifies the ways designating the place of novel VAR sources and/or settings of the VAR sources that are installed currently and the settings of facilities including on-load tap changers (OLTCs). Reactive power sources ordinarily consist of synchronous generators/condensers, reactor/capacitor banks, as well as flexible AC transmission systems (FACTS) controllers. It can be classified into two subjects as reactive source programming as well as reactive power dispatch. For reactive programming, the concerned temporal duration is the coming few months or years, and besides considering the optimum milieu of facilities that are installed currently, installation of novel reactive power sources is contemplated. It is performed in offline and online ways. The main purposes of offline reactive dispatch can be found in the duration of the coming few days or weeks, while, another model is carried out in the coming few minutes or hours. Opposing the reactive planning, both online and offline reactive power dispatches only designate the optimum settings of extant facilities. Optimal reactive power flow (ORPF) which is a specific instance of the optimal power flow (OPF) issue is an utterly significant instrument with regard to assured and gainful utilization of power systems. The OPF's control parameters have a proximate connection with the reactive power flow, including shunt capacitors/reactors, voltage magnitudes of generator buses, output of static reactive power compensators, transformer tap-settings. In the ORPF problem, the transmission power falloff is brought to a minimum and the voltage profile is modified and the operating and physical constraints are satisfied. Note that shunt capacitors/reactors and tap-settings of transformers are discrete variables while and except other variables are continuous. Hence, the reactive power dispatch issue is nonlinear, non-convex has equality and inequality limitations and has discrete and continuous variables.

7.1 Introduction

By the elevated exploitation as well as loading of the grid transmission system and besides because of refined enhanced operating conditions the issue of voltage stability and voltage collapse draws increasing consideration. A voltage drop could be taken in the power systems or subsystems and could emerge very suddenly [1]. Constant controlling of the system status is hence necessary. The reason of the 1977 New York blackout has been substantiated to be the reactive power issue. The 1987 Tokyo blackout was accepted to be because of reactive power deficit as well as a voltage drop at peak load in summer.

These facts have strongly shown that reactive power play an important role in the security of power systems as view of voltage stability. An appropriate compensation of system voltage profiles will improve the system securities in the operation and will decrease system losses [2]. The essential purpose of voltage regulation in the distribution system performance is to maintain the status voltage in the power system steady in the suitable scope. The desirable voltages could be acquired by either directly manipulating the voltage or reactive power flow which in its own right will influence the voltage collapse. The reactive tools usually employed for the voltage and reactive power control are on-load tap-changer (OLTC) transformers, steps voltage regulator and switched shunt capacitors [3, 4]. Such reactive tools are generally utilized on the basis of a presumption that power runs in just one direction and the voltage diminishes along the feeder, from the substation to the remote end.

An OLTC transformer is a transformer with automatically changeable taps. The OLTC is a section of most of HV/MV substation transformers [5]. A shunt capacitor produces reactive power to make up for the reactive power demand and hence increases the voltage. Shunt capacitors could be installed in the substation (hereinafter referred to as substation capacitors) or along the feeder (hereinafter referred to as feeder capacitors). A steps voltage regulator is an autotransformer with automatically adjustable taps that is ordinarily installed when the feeder is too long in such a manner which voltage regulation with OLTC and shunt capacitors is not enough. Voltage and reactive power control entails suitable coordination between the extant voltage and reactive power control equipment [6].

Many distribution network operators (DNOs) control these equipment locally via use of customary controllers to keep the voltages in the distribution system about approved range while bring to a minimum the voltage collapse and power falloffs. Various techniques have been presented in order to get better voltage and reactive power control in the distribution system for programming and operation stages. Within this time, many scholars have presented the trouble of voltage and reactive power control in distribution power systems through concentrating on automated distribution power system, with off-line setting control or real time control. The offline setting control intends to explore a dispatch program for OLTC movement and capacitor switching on the basis of day-ahead load prediction, in the meantime

the real time control endeavors to control the capacitor and OLTC on the basis of real time surveying and trainings [7]. The major difficulty in utilization of the off-line setting control way is its affiliation to remote control and communication links to all capacitors. Nonetheless, a lot of DNOs do not communicate with links that are downstream to the feeder capacitor locations.

In the other hand, the nature of modern power systems has changed due to a variety of factors: the increased demand for sustainability, rises in the price of oil and the need for the reduction of greenhouse gases, all of which have driven a large increase in the level of wind generation in the power system. The intergovernmental panel on climate change has cited that wind energy will be the primary source of renewable generation in the electricity sector [8]. Wind generation in both Europe and the United States is the dominant renewable resource currently present in power systems. In Europe, wind energy is set to triple in penetration by the year 2020, with 15.7% of the continent's total energy supplied by wind generation [9]. In the United States, there is currently 42,432 MW of installed capacity providing 2.3% of the U.S. electricity mix, with the number set to rise to 25% by the year 2025 [10]. With wind generation set to become a significant generation resource in power systems around the world, it will become increasingly important to fully understand its impacts and interaction with the conventional elements in power systems. In fact, the real power unit output is generally restricted by radius ($V_t I_a$), as follows

$$P_G^2 + Q_G^2 \leq (V_t I_a)^2 \tag{7.1}$$

Constrain of field is circular ($V_t E_f / X_s$) at ($0, -V_t^2/X_s$). It can be defined as

$$P_G^2 + \left(Q_G + \frac{V_t^2}{X_s}\right)^2 \leq \left(\frac{V_t E_f}{X_s}\right)^2 \tag{7.2}$$

where, P_G, Q_G, V_t, I_a, E_f and X_s are active power, reactive power, terminal voltage, armature current, Excitation voltage and Synchronous reactance of the synchronous generator, respectively.

Fundamentally, power systems have been designed and operated around the concept of generation delivery from large synchronous machines. These machines have high levels of reliability and complex control systems that allow the system to maintain high levels of operational security. The correct operation and control of these machines across the full spectrum of time-frames is critical for maintaining reliable power system operation and stability [11–13].

Maintaining voltage stability requires that the various components and elements of the system can interact without issue across all of the timeframes of the stability spectrum. Wind generation will have significant impact across the power system stability time-frame and as wind generation becomes a more common source of generation in the system, new mitigation techniques will be necessary to continue

operating the power system in an assured and stable way [14]. While the effect of reactive power reserves (RPRs) on system stability is widely acknowledged, few studies have been conducted to investigate how RPR levels could be used to indicate the amount of voltage stability margin (VSM) [15].

In contemporary years, certain papers with mathematical algorithms have been presented to think out the reactive power dispatch (RPD) problem [16–19]. These algorithms, including Non-linear Programming (NLP), Newton method, Gradient method, Linear Programming (LP), Jacobian matrix, Quadratic Programming (QP), interior point methods and so on, have been fruitfully used for thinking out the RPD problem. However, certain drawbacks are still linked to them. The RPD problem is non-linear, non-differential and non-convex problem with more than one local optimum, while these methods work based linearizing which make them less efficient in finding the global optimum. On the other hand, some of these methods suffer from special shortages, such as mathematical complexity and insecure convergence (NLP), piecewise quadratic cost approximation (QP), convergences to local optima (Newton method), a simplified piecewise linear estimate (LP), etc. Also, their optimization process mainly depends on the initial solution and can easily fall into local optima.

To overcome these disadvantages, different heuristic-based techniques are developed for solving the RPD problem. Population-based optimization techniques inspired by nature may be classed in two significant categories that are swarm intelligence and evolutionary algorithms. Many methods rooted in these techniques including fuzzy Adaptive Particle Swarm Optimization (FAPSO) [20], Real Genetic Algorithms (RGA) [21], Tabu Search (TS) [22], Particle Swarm Optimization (PSO) [23], Improved PSO (IPSO) [24], stochastic method [25], Hybrid Stochastic Search (HSS) [26], Differential Evolution (DE) [27], Artificial Bee Colony (ABC) [28] as well as other methods have been broadly employed in the problem of RPD. However, these methods appear to be proper approaches for the unravelment of the RPD variable optimization problem.

Attention to use optimization methods in distributed generation is increasing [29, 30]. In [31], an optimization method employed for wind power is offered, by a primal-dual predictor corrector interior point method, employed to explore the operating points of a single WT in a WF. The voltage stability based on reactive power control has been reviewed in rest of this chapter. The real transmission power loss minimization is consider as function, meantime the permitted transformer capacity, voltage range and conductor current capacity are added as the loading limitations. Moreover, OLTC operation and voltage fluctuation index are also analyzed. The reactive power in term of voltage stability is shown with reactive power control and local voltage in which timing of feeder capacitors are monitored and is still broadly employed.

7.2 Voltage Stability Based RPD Model

The different purposes of power system are sum of voltage deviations on load busses, system transmission falloffs, voltage stability, security, etc. Such purposes are contradictory in their essence and couldn't be dealt with by customary single purpose optimization techniques. Generally, the RPD model could be explained as follows in mathematical terms:
Problem Purposes

- *Purpose 1: Bringing to a minimum the total real power losses*

Transmission falloffs in the network can be stated as economic losses procuring no advantages. Thus, transmission falloffs are understood as a falloff in proceeds via the utility. The intensity of each falloff requires accurate estimation and applicable moves made to bring them to a minimum. When the transmission falloffs are stated with regard to bus voltages and associated angles, the falloffs could be stated based on Newton–Raphson as follows

$$J_1 = P_{loss}(x,u) = \sum_{k=1}^{N_L} g_k[V_i^2 + V_j^2 - 2V_iV_j\cos(\theta_i - \theta_j) \tag{7.3}$$

i and j end respectively if g_k is the conductance of the line i-j, V_i and V_j are line voltages and θ_i and θ_j are the line angles at the line. The k^{th} network branch is k. It connects bus i to bus j. If N_D is the set of numbers of power demand bus and j = 1,2, …, N_j where, N_j is the set of numbers of buses in adjacency with bus j, i = 1,2, …, N_D. P_G is the active power in line i and j. x and u are the dependent variables vectors and vector of control variables, respectively.

- *Objective 2: Bringing voltage deviation to a minimum*

Satisfying user's demands with the smallest expense with a desirable continuity of supply and sufficiently little deviation in voltage is the second function of one RPD problem. The following is its expression

$$J_2 = VD(x,u) = \sum_{i=1}^{Nd} |V_i - 1.0| \tag{7.4}$$

where, N_d is number of load buses.

- *Objective 3: Minimization of L-index voltage stability*

Voltage stability and voltage drop problem draws increasing attention by increasing the power transmission system loading and exploitation, a voltage collapse could

happen in systems or subsystems. And it could emerge very suddenly [15, 34]. *L-index*, L_j of the *j*th bus could be stated by means of below equation

$$\begin{cases} L_j = \left|1 - \sum_{i=1}^{N_{PV}} F_{ji} \frac{V_i}{V_j}\right|, j = 1, 2, \ldots, N_{PQ} \\ F_{ji} = -[Y_1]^{-1}[Y_2] \end{cases} \tag{7.5}$$

where, N_{PV} and N_{PQ} are numbers of *PV* and *PQ* buses, respectively. Y_1 and Y_2 are the Y_{BUS} system sub-matrices acquired following the segregation of *PQ* and *PV* bus parameters as shown in the below equation

$$\begin{bmatrix} Y_1 & Y_2 \\ Y_3 & Y_4 \end{bmatrix} \begin{bmatrix} V_{PQ} \\ V_{PV} \end{bmatrix} = \begin{bmatrix} I_{PQ} \\ I_{PV} \end{bmatrix} \tag{7.6}$$

where *L-index* is calculated for the whole load buses. L_j shows there weren't load case and voltage drop circumstances of bus *j* in a feasible numerical range of [0, 1]. Thus, a representative *L* delineating the fixedness of the complete system is formulated as follows

$$L = \max(L_j), j = 1, 2, \ldots, N_{PQ} \tag{7.7}$$

In the optimal RPD problem, incorrect tuning of continuous and discrete control variable settings might boost the *L-index* value, which may reduce the system voltage fixedness outskirt. Let the maximum value of *L-index* be denoted as $L_{\max}$. Therefore, to improve the voltage fixedness and to keep the system remote from the voltage drop margin, the formula for the succeeding purpose function will be as follows

$$J_3 = VL(x, u) = L_{\max} \tag{7.8}$$

Objective Constraints

- *Limitations 1: Equality Limitations*

Power balance is equality limitations. To rephrase, the total power generation (P_G) must cover the total demand (P_D) as well as total real power losses in transmission lines. Equality constraints of real and reactive power in each bus can be expressed as below

$$\begin{cases} P_{G_i} - P_{D_i} = V_i \sum_{j=1}^{N_B} V_j [G_{ij} \cos(\theta_i - \theta_j) + B_{ij} \sin(\theta_i - \theta_j)] \\ Q_{G_i} - Q_{D_i} = V_i \sum_{j=1}^{N_B} V_j [G_{ij} \sin(\theta_i - \theta_j) - B_{ij} \cos(\theta_i - \theta_j)] \end{cases} \tag{7.9}$$

where; N_B and Q_{Gi} are the numbers of buses and the reactive power produced for ith bus, respectively; P_{Di} and Q_{Di} are real and reactive power at the ith load bus, respectively; G_{ij} and B_{ij} are the transfer conductance and susceptance between bus i and bus j, respectively; V_i and V_j are the voltage intensities at bus i and bus j, respectively; and θ_i and θ_j are the voltage angles at bus i and bus j, respectively. The equality limitations in (7.9) are nonlinear equations which could be thought out by employing Newton-Raphson method to create an answer to the load flow problem. Within the duration of answering, the real power output of one generator, titled slack generator, remains to fill in the real power losses and satisfy the equality limitation in Eq. (7.9). The load flow answer produces all bus voltage intensities and angles. Therefore, the real power losses in transmission lines could be obtained using Eq. (7.3).

- *Limitation 2: Generation Capacity Limitations*

For solid performance, the generator reactive power and bus voltage can be constrained through lower and upper limits as below

$$Q_i^{\min} \le Q_i \le Q_i^{\max}, v_i^{\min} \le v_i \le v_i^{\max} \tag{7.10}$$

where, $Q_i^{\min}$, $Q_i^{\max}$, $v_i^{\min}$ and $v_i^{\max}$ are the minimal and maximal value for reactive power and voltage magnitude of the ith transmission line, respectively. A clarified input/ output curve of the thermal unit understood as heat rate curve is indicated in Fig. 7.1.

- *Limitation 3: Line flow Limitations*

A significant limitation of RPD problem is the line limitation. Since any line has a constrained capacity for current power, the constraint should be checked following the power system load flow. For that reason, this section argued the answer for RPD problem with line flow limitations. The following is the modeling of this constraint

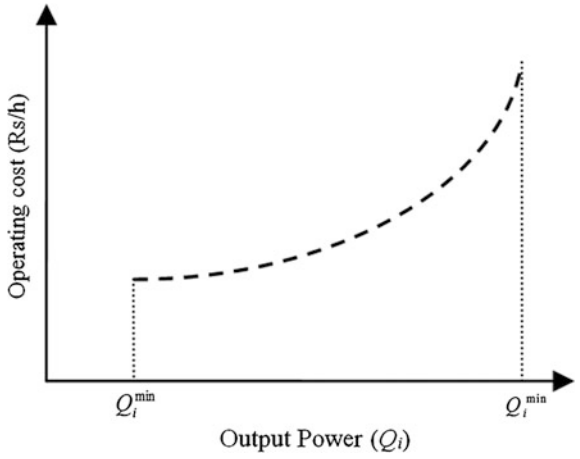

Fig. 7.1 Operating expenses curve for one generator

$$\left|S_{Lf,k}\right| \leq S_{Lf,k}^{\max}, k = 1, 2, \ldots, L \tag{7.11}$$

where $S_{Lf,k}$ is the real line k power flow; $S_{Lf,k}^{\max}$ is the upper limit of power flow of line k. L is the number of transmission lines [3].

- *Constraints 4: Discrete control variables*

The shunt susceptance (B_{sh}) and transformer tap settings (T_i) values are taken as discrete values. These must be constrained by their lower and upper limits as below

$$\begin{cases} T_i^{\min} \leq T_i \leq T_i^{\max} \\ B_{sh_i}^{\min} \leq B_{sh_i} \leq B_{sh_i}^{\max} \end{cases} \tag{7.12}$$

Problem formulation
Adding up the entire purpose performances and the equality and inequality limitations, a nonlinear limited multi-purpose optimization problem in mathematical terms could be the formula for the RPD problem, which can be represented by

$$\begin{aligned} & J_{Final} = \min_{P_G}[VL(x,u), P_{loss}(x,u), VD(x,u)] \\ & \text{s.t. :} \\ & g(x,u) = 0 \\ & h(x,u) \leq 0 \\ & x^T = [[V_L]^T, [S_L]^T, [Q_G]^T] \\ & u^T = [[V_G]^T, [Q_C]^T, [T]^T] \\ & J_{Final} = \min_{P_G}[VL(x,u), P_{loss}(x,u), VD(x,u)] \end{aligned} \tag{7.13}$$

where, g and h are the equality and inequality limitations, respectively. $[V_L]$, $[Q_G]$ and $[S_L]$ are the vectors of load bus voltages, generator reactive power outputs and the transmission line loadings, respectively. $[V_G]$, $[T]$ as well as $[Q_C]$ are the vectors of generator bus voltages, transformer taps and reactive compensation instruments, respectively.

7.3 Reactive Power Capacity and Control Options in Wind Farms

The requisite of the membership of WFs in grid control matters has increased the inclusion of power electronics and the expansion of new WT generation concepts, leading to variable speed wind turbines [30]. The most popular wind generation technology employed among them today is the DFIG. In this study, the DFIG

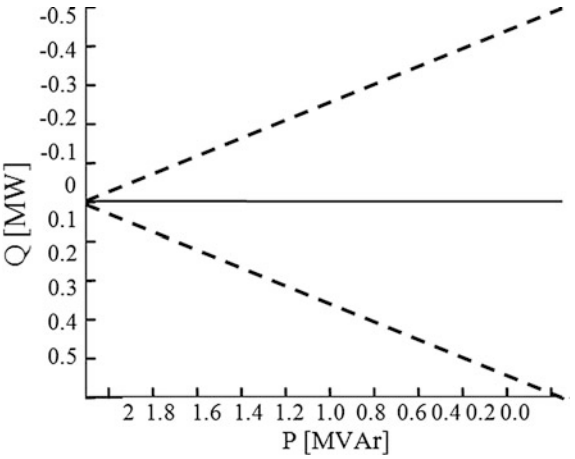

Fig. 7.2 *Q* property of an individual WT appertaining to G80-2.0 MW

Table 7.1 Properties of wind power

Parameter	Value	Parameter	Value
Diameter	80 m	PN	2.1 MW
Rotational speed	1680 rpm	Voltage	0.68 kV
Type	DFIG	Power factor	0.978 CAP–0.957 IND

technology is employed. The capacity of reactive power injection into the grid generally is associated to the used control approach, the active power generation and the converter size. The P-Q quality of the WTs employed in this study is given in Fig. 7.2. Specifically, it shows the business wind generator Gamesa WT G80-2.0 MW [26]; the useful data are given in Table 7.1. This WT acts with Power Factor (*PF*) 0.98 capacitive and 0.96 inductive. Consequently, the reactive power capability is bounded relying on the active power production. Its reactive power capacity is shown with the WT's trait and the influences of lines as well as cables. Thus, the WFP-Q trait is analogous to the same for the WTs. However, it's oriented to the capacitive side, as displayed in Fig. 7.3.

The green line shows the *PQ* trait of WF for $PF = 1$. For a power production less than 10 MW, the cable influence is larger than the transformer influence, since the transformer influence is paramount for large output power from WF. Thus, novel consumption and production of WF areas are modeled, for a range in which the WF alters the reactive power requisites exists. If the WF gets a capacitive reactive power in the small active power production range, the WTs set point will alter to be inductive. Voltage control can be performed via reactive power injection as well as transformer taps, like the way it is given in Table 7.2.

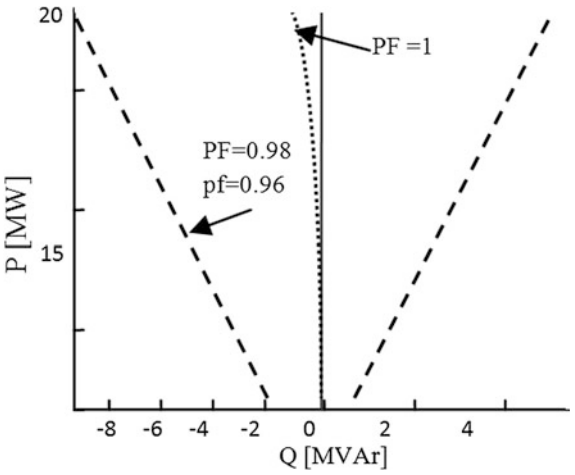

Fig. 7.3 Q property of the tested WF comprised of twelve G80-2.0 MWWTs, with no compensation gear

Table 7.2 Voltage and reactive power control alternatives in wind farms

Model	Control variable			
	Reactive power	Voltage	Discrete (Dis)/Continuous (Con)	Response time
Capacitor	●		Dis	Slow
STATCOM	●		Con	Fast
SVC	●		Con	Fast
DFIG	●		Con	Fast
Sync	●		Con	Fast
Tap		●	Dis	Slow

7.3.1 Objective Function

As the WF has to be capable to acquire reactive power from the grid, the optimum handle or reactive power resources in the WF must be handled. For optimizing the RPD among WTs and the control of various equipment like STATCOM or capacitor bank, one HBMO algorithm can be used. This fitness is given to bring the active power drops to a minimum along the WF cables or lines

$$\min J(Var_x, Var_y) = \min P_{losses} \tag{7.14}$$

where, Var_y denote the transformer tap location, the STATCOM reactive power setting and the capacitor bank state as independent variables, and Var_x represent the dependent variables that are the single WT reactive power outputs.

The control parameters are given by a j-dimensional vector, where j is the number of the enhanced variables. Meanwhile, any vector denotes one solution. i solutions exist and each one is a nominee answer.

7.3.2 Objective Constraints

The reactive power of each WT, tab of transformers and the STATCOM reactive power are constrained by

$$Var_{WT_i}^{\min} \leq Var_{WT_i} \leq Var_{WT_i}^{\max}, i = 1, 2, \ldots, N_G \tag{7.15}$$

$$T_i^{\min} \leq T_i \leq T_i^{\max} \tag{7.16}$$

$$Var_{Statcom}^{\min} \leq Var_{Statcom} \leq Var_{Statcom}^{\max} \tag{7.17}$$

Moreover, an additional equality limitation exists. The reactive power prerequisite in Point of Common Coupling (PCC) for the voltage control task can be modeled as an equality limitation by

$$Var_{PCC}^{*} = Var_{PCC}^{meas} \tag{7.18}$$

Within this study, the exploration of possible answers is employed to certificate an answer which meets the limitations that can be defined as follows

$$SO_i^{k+1} = \begin{cases} SO_i^k + v_i^{k+1}, & SO_i^{\min} \leq SO_i^k + v_i^{k+1} \leq SO_i^{\max} \\ SO_i^{\max}, & SO_i^k + v_i^{k+1} > SO_i^{\max} \\ SO_i^{\min}, & SO_i^{\min} > SO_i^k + v_i^{k+1} \end{cases} \tag{7.19}$$

With Eq. (7.9), the inequality restraints are met, the equality restraint (7.18) still needs to be answered. Because in the WF the main elements influencing the reactive power flow are the reactive power consumption of transformers, a scheme for meeting the equality constraint is introduced. Yet, bearing in mind the goal to

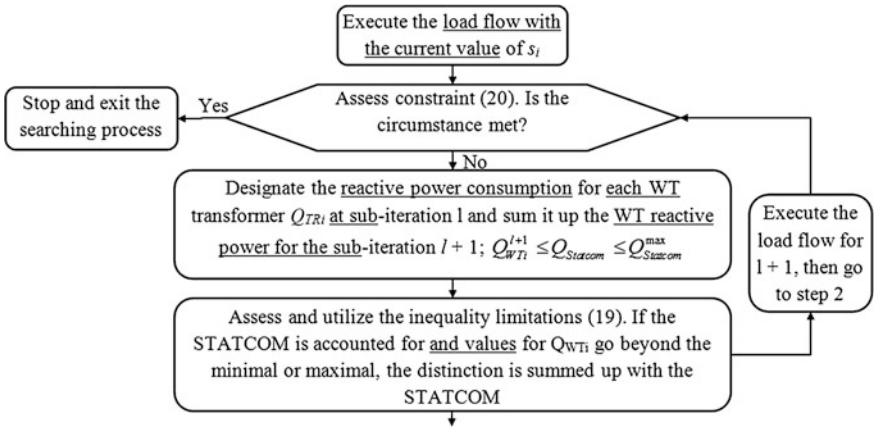

Fig. 7.4 Flowchart for the possible answer exploration process

decrease the searching CPU time to explore a possible answer, the equality constrain is improved and an error value ε is modeled.

$$\left|Var_{PCC}^{*} - Var_{PCC}^{meas}\right| < \varepsilon \tag{7.20}$$

This strategy is given in Fig. 7.4.

7.4 Voltage Stability Based RPP Model

Voltage deviation and stability limited VAr programming or Reactive Power Planning (RPP) is a significant demanding effect in power systems [32]. Investigations on voltage fixedness are fundamentally related to reactive power compensation sources. Having adequate reactive power compensation sources, principally in the shunt connection, the voltage stability boundary could be boosted a lot to make sure of system security [33]. Thus, appropriate programming of reactive power is a serious matter because of its specialized harness and the large expense of relocating a shunt compensator in economic terms when that is assembled. As an important demanding problem in power system research, RPP or VAr programming is a mixed integer nonlinear optimization programming with a huge scale of optimal variables [34]. The VAr programming is delineated in this part of applicable operational account limitations at various load levels. The mathematic formulation of optimization-based RPP model via accounting for voltage fixedness limitation could be stated as follows

$$\begin{aligned}
&\min\ \alpha \sum_{k=1,\ldots,N_L} P_{loss}^{(k)} + \beta \sum_{i=1,\ldots,N} Q_{ci} y_i + \gamma \sum_{i=1}^{Nd} \left|V_i - V_i^0\right|, \text{s.t.:} \\
&\sum_{i=1}^{N} y_i = N_c \\
&P_{G_i}^{(k)} - P_{L_i}^{(k)} - V_i^{(k)} \sum_{jw_i} V_j^{(k)} \times \left(G_{ij}\cos\theta_{ij}^{(k)} + B_{ij}\sin\theta_{ij}^{(k)}\right) = 0 \\
&Q_{G_i}^{(k)} + Q_{C_i}^{(k)}(y_i) - Q_{L_i}^{(k)} - V_i^{(k)} \sum_{jw_i} V_j^{(k)} \times \left(G_{ij}\sin\theta_{ij}^{(k)} - B_{ij}\cos\theta_{ij}^{(k)}\right) = 0 \\
&V_{i\min}^{(k)} \le V_i^{(k)} \le V_{i\max}^{(k)}, -S_{ij\max}^{(k)} \le S_{ij}^{(k)} \le S_{ij\max}^{(k)} \\
&P_{G_i\min}^{(k)} \le P_{G_i}^{(k)} \le P_{G_i\max}^{(k)}, i \in NG \\
&Q_{C_i\min}^{(k)} \le Q_{C_i}^{(k)} \le Q_{C_i\max}^{(k)}, i \in NG \\
&P_{tieline}^{(k)} \le TTC(Q_C^{(k)})
\end{aligned} \tag{7.21}$$

and,

$$P_{loss}^{(k)} = \sum g_{ij}\left((V_i^{(k)})^2 + (V_j^{(k)})^2 - 2V_i^{(k)}V_j^{(k)}\cos\theta_{ij}^{(k)}\right) \tag{7.22}$$

where, NG, N, N_L and N_c, are number of generators, number of buses, number of operation load levels and number of VAr sources which must be installed, respectively.

Subscript k indicates different load levels which $k = 1,\ldots, N_L$. $T^{(k)}$, α, β and y_i are the time period of load level kth year, the energy expense per kWh, the calculated mean yearly preservation and assignment expense and binary variable (y_i = 1" if the VAr tool is installed at bus i, or else, "0"), respectively. PG_i, QG_i, PL_i, and QL_i are the generator active outputs, reactive power outputs, the load active and reactive power demands at bus i, respectively. S_{ij}^k is the line flow of line i-j where load level is k; other than for the value of zero, Q_{ci} is housed in a certain VAr capacity interval at bus i, Q_{ci}^k is the VAr capacity needed at load level k, and Q_{ci} is the ultimate VAr size at bus i; $P_{tieline}$ is the total active power flow with the tie lines from the source zone to sink zone; $TTC(Q_c^{(k)})$ is a piecewise linear interpolation function employed as static voltage fixedness limitation to be delineated later in this research, and Q_c is the Q_{ci} set at all nominee buses.

The Eq. (7.3) brings the yearly expense of power system, voltage deviation and real falloffs plus VAr tool to a minimum. Nonetheless, additional purposes could be accounted for namely bringing generation expense and VAr installation expense, etc. to a minimum However, such points do not alter the point of focus in this study, and other purpose performances could be accounted for if it is needed in a certain power system. The mentioned VAr programming plane is static voltage stability (SVS) limited OPF model. The important cause for the computational demand of the voltage fixedness limited OPF model is the requisite of two constraints and variables sets associated to the regular performance and drop points [32]. The two variables sets offer a demand to answer the optimization model, particularly for a huge power system having several conditions. To depict this demand, TTC could be employed to roughly offer the SVS limitation. At a stable VAr compensation model by accounting for certain plausible conditions that are clarified in advance, the security limited TTC optimization model is given by

$$
\begin{aligned}
&\min_k \left\{ \max \sum_{\substack{i \in Source\,Area \\ j \in Sink\,Area}} (P_{ij}^{(k)} - P_{ij0}) \right\}, \text{s.t.:} \\
&\sum_{i=1}^{N} y_i = N_c \\
&P_{G_i}^{(k)} - P_{L_i}^{(k)} - V_i^{(k)} \sum_{jw_i} V_j^{(k)} \times (G_{ij} \cos\theta_{ij}^{(k)} + B_{ij} \sin\theta_{ij}^{(k)}) = 0 \\
&Q_{G_i}^{(k)} + Q_{C_i}^{(k)}(y_i) - Q_{L_i}^{(k)} - V_i^{(k)} \sum_{jw_i} V_j^{(k)} \times (G_{ij} \sin\theta_{ij}^{(k)} - B_{ij} \cos\theta_{ij}^{(k)}) = 0 \\
&V_{i\min}^{(k)} \le V_i^{(k)} \le V_{i\max}^{(k)}, -S_{ij\max}^{(k)} \le S_{ij}^{(k)} \le S_{ij\max}^{(k)} \\
&P_{G_i\min}^{(k)} \le P_{G_i}^{(k)} \le P_{G_i\max}^{(k)}, i \in \text{Source Area} \\
&Q_{C_i\min}^{(k)} \le Q_{C_i}^{(k)} \le Q_{C_i\max}^{(k)}, i \in \text{Source Area} \\
&\frac{P_{Li}^{(k)}}{P_{Li}^{0}} = \frac{Q_{Li}^{(k)}}{Q_{Li}^{0}}, i \in \text{Sink Area}
\end{aligned}
\tag{7.23}
$$

where, Q_{Li}^{0} and P_{Li}^{0} are the base case reactive and real power demands at load bus i, respectively. P_{ij0} expresses the base case power flow between line i-j; and $P_{ij}^{(k)}$ indicates the line flow of line i-j, having Var compensation. Meanwhile, the superscript $k = 1,\ldots, N_{cntg}$, characterizes various performance statuses with the regular performance, and $k > 0$ characterizing the post-condition statuses for the kth condition phenomenon.

7.5 Simulation

A. Voltage stability in wind farm

Wind Energy is one of the greatly encouraging renewable energy sources in Mongolia. WF within Inner Mongolia owns 200 wind turbines which are broken down into 20 sets, and there are 10 turbines in any set. The total installed capacity is as high as 300 MW. The wind turbine increases to 35 kV by box-type transformer T2, afterwards by 20 35 kV coupled transmission lines to the substation, which is comprised of two principal parts of the 220 kV transformer step-up substation.

There are 403 nodes in the wind farm model, because of its sophistication and restricted area [35], only 42 nodes were selected as shown in Fig. 7.5. To account for cable lines losses, Static VAr compensation (SVC) is installed in the nodes for simulation. By computing the wind farm in the network, the optimum reactive compensation could be answered. Reference power SB is 100 MW, reference voltage is 220 kV, and the largest reactive investment is 500 million.

Encrypt the SVC and on-load tap modifier. 50 is the highest code, and 100 is the highest number of disasters. Table 7.3 shows the compared *of* reactive power optimization between Traditional Genetic Algorithm (TGA), Improved Genetic Algorithm (IGA) and Honey Bee Mating Optimization (HBMO). The IGA reduces the network losses and financing of compensation gear. And it's more appropriate than TGA.

B. Voltage stability founded on RPP

The IEEE 118-bus system [37, 38] is employed for case study, as indicated in Fig. 7.6. This power system is altered by decreasing maximal generator reactive power output and boosting reactive load, as indicated in Tables 7.4 and 7.5. This adjustment is employed in order to build the system stressed enough in the manner that the reactive power compensation is required. Therefore, the voltage intensity at bus 30 in the altered system is less than 0.944 p.u. in the case with heavy loading. The altered system information are employed as the "heavy-load" case. Afterwards, loads are moved down by 0.78 to construct the "medium-load" case, and moved down more by 0.76 to make the "light-load" case. In the total 8760 h yearly, heavy-load and light-load cases are presumed to be 1200 h each condition, and therefore, the medium-load case gets 6360 h. α, β and χ are 40 $/MWh, 3600 $/year and 6400 kV for each VAr tool.

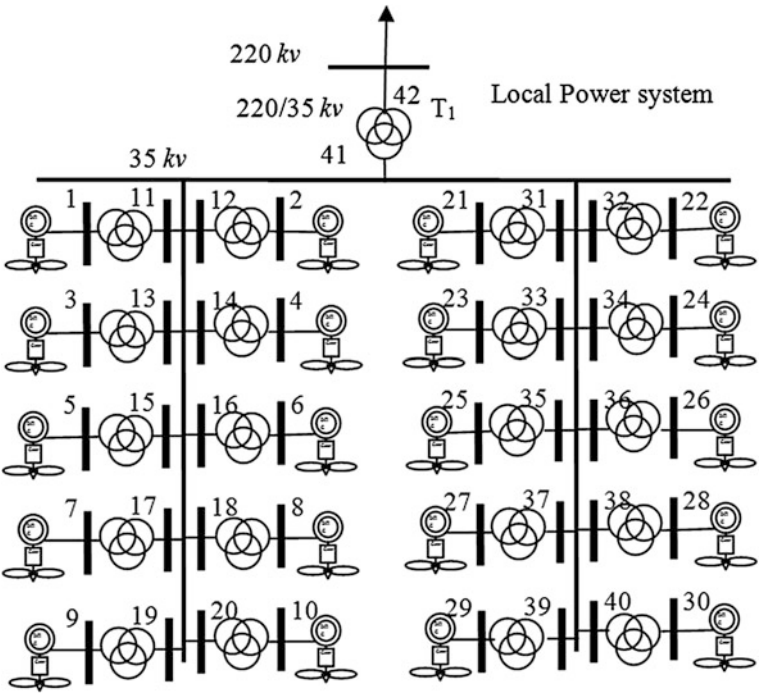

Fig. 7.5 The model of the wind farm having 42 nodes

Table 7.3 Contrasted conclusions of reactive power optimization in wind farms

Project	Financing of reactive power compensation (million Yuan)	The system falloff (kW)		
		V = 4 m/s	V = 8 m/s	V = 12 m/s
TGA [36]	338	1872	2480	3129
IGA [36]	336	1731	2292	2892
HBMO [1]	311	1721	2282	2671

In this section, certain indices founded on voltage fixedness are indicated to mention new nominee VAr tools. Furthermore, we must employ the indices that could provide data at all load buses. Hence, three indices constituted voltage and voltages fixedness associated information of any bus to appear in the index dataset matrix for fuzzy grouping. They are *L-index*, H/H_0 *Index*, and ultimately a voltage fluctuation index.

(1) H/H_0 *Index:* This index formulated in Eq. (7.24), is used to grant the test system delicate bus associated data.

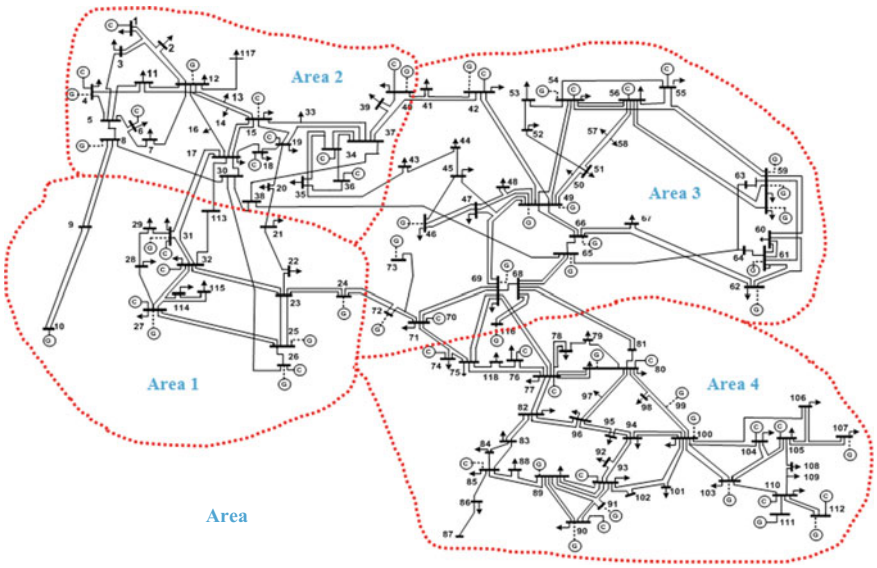

Fig. 7.6 IEEE 118-bus system

Table 7.4 Altered reactive load demand in the IEEE 118-bus system

PQ bus no	*Q* MVar	*PQ* bus no	*Q* MVar	*PQ* bus no	*Q* MVar
2	24	30	5	57	17
3	43	33	26	58	17
5	6	35	36	60	83
7	24	37	5	63	5
9	5	38	4	64	5
11	75	39	36	67	33
13	39	41	45	68	5
14	19	43	21	71	5
16	30	44	21	75	51
17	17	45	58	78	72
20	23	47	32	79	41
21	19	48	24	81	5
22	15	50	21	82	55
23	13	51	21	83	25
28	21	52	23	84	16
29	28	53	28	86	26

Table 7.5 Altered generator maximal reactive power output

Gen no	$Q_{G\max}$	Gen no	$Q_{G\max}$	Gen no	$Q_{G\max}$
1	12	42	295	80	277
4	295	46	95	85	19
6	46	49	205	87	997
8	295	54	295	89	297
10	195	55	18	90	297
12	115	56	10	91	97
15	25	59	175	92	5
18	45	61	295	99	96
19	20	62	15	100	151
24	296	65	195	103	36
25	136	66	195	104	19
26	996	69	295	105	19
27	296	70	27	107	197
31	296	72	97	110	19
32	38	73	97	111	997
34	21	74	5	112	997
36	21	76	17	113	197
40	295	77	67	116	997

$$\frac{H}{H_0} = \left[\frac{H_1}{H_{01}}, \ldots, \frac{H_k}{H_{0k}}\right] \tag{7.24}$$

where, H and H_0 are base case voltage intensity vectors at each bus and the voltage intensity with all loads adjusted to 0 for the power system [39].

(2) *L-Index:* With the boosted loading and utilization of the power transmission system and also because of enhanced optimized performance, the issue of voltage fixedness and voltage drop draw increasing attention. A voltage drop could happen in systems or subsystems and could emerge very suddenly. *L-index*, L_j of the *j*th bus could be stated by using the equation below

$$\begin{cases} L_j = \left|1 - \sum_{i=1}^{N_{PV}} F_{ji}\left(\frac{V_i}{V_j}\right)\right| \\ [Y_1] \times F_{ji} = -[Y_2], j = 1, 2, \ldots, N_{PQ} \end{cases} \tag{7.25}$$

where, N_{PV} and N_{PQ} are number of PV and PQ bus, respectively. Parameters Y_1 and Y_2 are the system Y_{BUS} sub-matrices acquired following segregating the PQ and PV bus bar parameters as shown in Eq. (7.26)

$$\left\{ \begin{bmatrix} Y_1 & Y_2 \\ Y_3 & Y_4 \end{bmatrix} = \begin{bmatrix} I_{PQ} \\ I_{PV} \end{bmatrix} \times \begin{bmatrix} V_{PQ} \\ V_{PV} \end{bmatrix}^{-1} \right\} \tag{7.26}$$

where *L-index* is computed for the entire load buses and L_j indicates no load case and voltage drop circumstances of bus j in a possible numerical range of (0, 1).

(3) *Bringing voltage deviation to a minimum:* The three index of an RPP problem is to satisfy consumer's demands with the lease expense with a desirable expectance of persistence of supply and adequately little voltage deviation. It can be stated as

Table 7.6 Three indices employed for fuzzy grouping algorithm

PQ bus no	*L*-index	H/H_0	Voltage fluctuation (%)	*PQ* bus no	*L*-index	H/H_0	Voltage fluctuation (%)
2	0.9554	1.0441	1.4252	57	0.9552	1.0222	1.6092
3	0.9577	1.0431	1.6084	58	0.9519	1.0356	1.0193
5	0.9543	1.0721	1.6271	60	0.9728	1.0523	1.3364
7	0.9540	1.0692	1.5476	63	0.9765	1.0223	1.1155
9	0.9762	1.0561	1.0672	64	0.9627	1.0522	1.6726
11	0.9672	1.0365	1.1797	67	0.9512	1.0623	1.4891
13	0.9663	1.0702	1.2301	68	0.9573	1.0111	1.3433
14	0.9540	1.0454	1.4635	71	0.9603	1.0112	1.3234
16	0.9751	1.0302	1.0932	75	0.9540	1.0228	1.0472
17	0.9684	1.0821	1.4954	78	0.9521	1.0091	1.0253
20	0.9605	1.0761	1.0731	79	0.9521	1.0022	1.7192
21	0.9654	1.0456	1.4490	81	0.9521	1.0435	1.0451
22	0.9620	1.0541	1.3393	82	0.9692	1.0074	1.3584
23	0.9522	1.0510	1.5352	83	0.9723	1.0234	1.0665
28	0.9571	1.0181	1.4912	84	0.9693	1.0692	1.5623
29	0.9535	1.0261	1.6224	86	0.9632	1.0024	1.5616
30	0.9555	1.0413	1.6123	88	0.9664	1.0806	1.4963
33	0.9572	1.0211	1.2296	93	0.9585	1.0646	1.1035
35	0.9625	1.0727	1.4875	94	0.9723	1.0425	1.4534
37	0.9513	1.0162	1.1354	95	0.9534	1.0527	1.3557
38	0.9771	1.0196	1.0218	96	0.9723	1.0225	1.6687
39	0.9782	1.0149	1.5113	97	0.9529	1.0392	1.4454
41	0.9647	1.0197	1.3435	98	0.9630	1.0833	1.5493
43	0.9641	1.0378	1.3297	101	0.9682	1.0473	1.3134
44	0.9601	1.0272	1.6215	102	0.9728	1.0452	1.2973
45	0.9772	1.0813	1.4145	106	0.9523	1.0229	1.5662
47	0.9611	1.0374	1.4273	108	0.9779	1.0422	1.0548
48	0.9533	1.0161	1.5944	109	0.9733	1.0541	1.0915
50	0.9730	1.0751	1.5528	114	0.9642	1.0590	1.1195
51	0.9610	1.0873	1.3926	115	0.9632	1.0342	1.2683
52	0.9570	1.0382	1.1283	117	0.9633	1.0321	1.5714
53	0.9620	1.0094	1.1636	118	0.9578	1.0864	1.5515

$$J_2 = VD(x,u) = \sum_{i=1}^{Nd} |V_i - V_i^{sp}| \tag{7.27}$$

where, N_d is number of load buses. The fuzzy grouping technique is first performed for the heavy load case by employing three various kinds of indices: *L-index*, H/H_0 index, and the voltage fluctuation index. Particularly, the voltage fluctuation manifests the relative deviation of the voltage intensity at the maximal TTC between zones 2 and 4 from the voltage intensity at the base operation case. Table 7.6 indicates the value of the indices at *PQ* buses, and Fig. 7.7 demonstrates post-standardization indices.

Because ordinarily more than one nominee location is available for installation of VAr (particularly in huge-scale power system), the least four values for any index are analyzed. The six weakest buses are {79, 78, 81, 37, 67, 23} on the basis of *L-index*, buses {79, 76, 82, 78, 53, 68} on the basis of H/H_0 index, and buses {79, 58, 38, 78, 81, 75} employing the voltage fluctuation index. Based on graphical review, the indices do not create identical assessment for the whole buses, which could similarly be observed from Fig. 7.7.

To explore an all-out exploitation of all the indices, it is mandatory to bring in the fuzzy theory to cluster the weak load buses. The whole PQ buses in the test system are contained in the fuzzy grouping procedure. The fuzzy clustering method categorizes the whole load buses into three sets that are: {79}; {78, 76, 81}; {other PQ buses}. From the perspective of voltage intensities, Bus 79 has both the least base-case voltage intensity and the maximum voltage fluctuation, therefore it finally

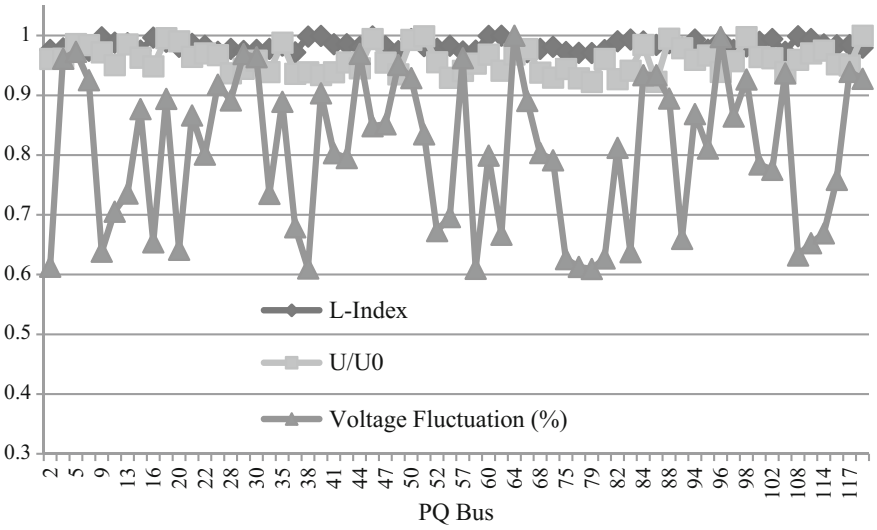

Fig. 7.7 Values of three indices after standardization

differentiates itself from the entire other buses. Furthermore, Buses 78, 76 and 81 are weak buses possessing resembling properties categorized in the second group. From the conclusions of the fuzzy grouping algorithm, Buses 30, 78, 76, and 81 are selected as nominee buses for novel VAr tools.

7.6 Conclusion

In this chapter, different models of reactive power dispatch/control system has been illustrated to minimize instability of bus voltage and generators using coordinate and optimal design of the generator voltages, transformers, switchable reactors and capacitors. Control of bus voltage has been shown to modify the reactive power aims and overtake them via the communication power system to the simulator. The RPD problem is implemented based on the active power aims place by active dispatch software.

Examinations of voltage fixedness are basically associated to reactive power compensation sources. Having sufficient reactive power compensation sources, mainly in the shunt connection, the voltage fixedness confine could be much booted to make sure of system security. This chapter solves the voltage stability as view of reactive power control problem by accounting for conditions and various load levels. In other words, this chapter offers voltage fixedness in customary distribution systems. Reactive power transmission, various voltage unstableness mechanisms and the static and dynamic reactive power sources role in various voltage unstableness mechanisms are examined. The chapter commences with a sketch of understood conclusions to update the audience's knowledge. Afterwards, the case study will demonstrate certain significant characteristics of the voltage fixedness concept in distribution systems. Moreover, reactive power dispatch in the wind farm is debated. It shows voltage stability with wind farm is better if correctly models its uncertainties.

References

1. A. Ghasemi, K. Valipour, A. Tohidi, Multiobjective Optimal Reactive Power Dispatch Using a New Multiobjective Strategy, Electrical Power and Energy Systems, vol. 57, pp. 318–334, 2014.
2. K. Ayana, U. Kilic, Artificial Bee Colony Algorithm Solution for Optimal Reactive Power Flow, Applied Soft Computing, vol. 12, pp. 1477–1482, 2012.
3. T.A. Short, Electric Power Distribution Handbook, CRC Press LLC, 2004.
4. T. Gonen, Electric Power Distribution System, McGraw-Hill Book Company, 1986.
5. M. Paramasivam, A. Salloum, V. Ajjarapu, V. Vittal, N.B. Bhatt, S. Liu, Dynamic Optimization Based Reactive Power Planning to Mitigate Slow Voltage Recovery and Short Term Voltage Instability, IEEE Trans. Power Syst., vol. 28, no. 4, pp. 3865–3873, Nov. 2013.
6. C.W. Taylor, Power System Voltage Stability, New York, NY, USA: McGraw-Hill, 1994.

7. B. Zhou, K.W. Chan, T. Yu, C.Y. Chung, Equilibrium-Inspired Multiple Group Search Optimization with Synergistic Learning for Multiobjective Electric Power Dispatch, IEEE Trans. Power Syst., vol. 28, no. 4, pp. 3534–3545, Nov. 2013.
8. M. Zare, T. Niknam, A New Multiobjective for Environmental and Economic Management of Volt/Var Control Considering Renewable Energy Resources, Energy, vol. 55, pp. 236–252, 2013.
9. D.S.B. Alencar, D.A.A. Marcio Formiga, Multiobjective Optimization and Fuzzy Logic Applied to Planning of the Volt/Var Problem in Distributions Systems, IEEE Trans. Power Syst., vol. 25, no. 3, pp. 1274–1281, 2010.
10. T. Niknam, M. Zare, J. Aghaei, Scenario Based Multiobjective Volt/Var Control in Distribution Networks Including Renewable Energy Sources, IEEE Trans Power Deliv., vol. 27, no. 4, pp. 2004–2019, 2012.
11. A. Ghasemi, H. Shayeghi, H. Alkhatib, Robust Design of Multimachine Power System Stabilizers Using Fuzzy Gravitational Search Algorithm, Electrical Power and Energy Systems, vol. 51, pp. 190–200, 2013.
12. G. Rogers, Power System Oscillations, 1st Ed, Springer, 1999.
13. H. Shayeghi, A. Ghasemi, A Multiobjective Vector Evaluated Improved Honey Bee Mating Optimization for Optimal and Robust Design of Power System Stabilizers, Electrical Power and Energy Systems, vol. 62, pp. 630–645, 2014.
14. M. Noshyar, H. Shayeghi, A. Talebi, A. Ghasemi, N.M. Tabatabaei, Robust Fuzzy-PID Controller to Enhance Low Frequency Oscillation Using Improved Particle Swarm Optimization, International Journal on Technical and Physical Problems of Engineering (IJTPE), vol. 5, no. 1, pp. 17–23, 2013.
15. A. Ghasemi, M.J. Golkar, A. Golkar, M. Eslami, Reactive Power Planning Using a New Hybrid Technique, Soft Comput., vol. 20, pp. 589–605, 2016.
16. K.Y. Lee, Y.M. Park, J.L. Ortiz, A United Approach to Optimal Real and Reactive Power Dispatch, IEEE Trans. Power Appar. Syst. PAS, vol. 104, no. 5, pp. 1147–1153, 1985.
17. S. Granville, Optimal Reactive Power Dispatch through Interior Point Methods, IEEE Trans. Power Syst., vol. 9, no. 1, pp. 98–105, 1994.
18. N.I. Deeb, S.M. Shahidehpour, An Efficient Technique for Reactive Power Dispatch Using a Revised Linear Programming Approach, Int. J. Electr. Power Syst. Res., vol. 15, pp. 121–134, 1988.
19. N. Grudinin, Reactive Power Optimization Using Successive Quadratic Programming Method, IEEE Trans. Power Syst., vol. 13, no. 4, pp. 1219–1225, 1998.
20. Z. Wen, L. Yutian, Multiobjective Reactive Power and Voltage Control Based on Fuzzy Optimization Strategy and Fuzzy Adaptive Particle Swarm, Int. J. Electr. Power Energy Syst., vol. 30, pp. 525–532, 2008.
21. Q.H. Wu, Y.J. Cao, J.Y. Wen, Optimal Reactive Power Dispatch Using an Adaptive Genetic Algorithm, Int. J. Electr. Power Energy Syst., vol. 20, no. 8, pp. 563–569, 1998.
22. D. Nualhong, S. Chusanapiputt, S. Phomvuttisarn, S. Jantarang, Reactive Tabu Search for Optimal Power Flow under Constrained Emission Dispatch, Proc. Tencon., pp. 327–330, 2004.
23. H. Yoshida, K. Kawata, Y. Fukuyama, S. Takayama, Y. Nakanishi, A Particle Swarm Optimization for Reactive Power and Voltage Control Considering Voltage Security Assessment, IEEE Trans. Power Syst., vol. 14, no. 4, pp. 1232–1239, 2000.
24. L.D. Arya, L.S. Titare, D.P. Kothari, Improved Particle Swarm Optimization Applied to Reactive Power Reserve Maximization, Int. J. Electr. Power Energy Syst., vol. 32, pp. 368–374, 2010.
25. Z. Hua, X. Wang, G. Taylor, Stochastic Optimal Reactive Power Dispatch: Formulation and Solution Method, Int. J. Electr. Power Energy Syst., vol. 32, pp. 615–621, 2010.
26. D.B. Das, C. Patvardhan, Reactive Power Dispatch with a Hybrid Stochastic Search Technique, Int. J. Electr. Power Energy Syst., vol. 24, pp. 731–736, 2002.
27. D. Karaboga, S. Okdem, A Simple and Global Optimization Algorithm for Engineering Problems: Differential Evolution Algorithm, Turk. J. Electr. Eng., vol. 12, no. 1, 2004.

28. K. Ayana, U. Kilic, Artificial Bee Colony Algorithm Solution for Optimal Reactive Power Flow, Appli Soft Compu., vol. 12, pp. 1477–1482, 2012.
29. P. Vovos, A. Kiprakis, A. Wallace, G. Harrison, Centralized and Distributed Voltage Control: Impact on Distributed Generation Penetration, IEEE Trans Power Syst., vol. 22, no. 1, pp. 476–83, 2007.
30. J.K. Kaldellis, K.A Kavadias, A.E. Filios, A New Computational Algorithm for the Calculation of Maximum Wind Energy Penetration in Autonomous Electrical Generation Systems, Appl. Energy, vol. 86, pp. 1011–23, 2009.
31. R. Almeida, E. Castronuovo, J. Lopes, Optimum Generation Control in Wind Parks When Carrying out System Operator Requests, IEEE Trans Power Syst., vol. 21, no. 2, pp. 718–25, 2006.
32. A. Monica, A. Hortensia, A.O. Carlos, A Multiobjective Approach for Reactive Power Planning in Networks with Wind Power Generation, Renewable Energy, vol. 37, pp. 180–191, 2012.
33. H. Amaris, M. Alonso, Coordinated Reactive Power Management in Power Networks with Wind Turbines and Facts Devices, Energy Conversion and Management, vol. 52, no. 7, pp. 2575–2586, 2011.
34. S. Ramesha, S. Kannan, S. Baskar, Application of Modified NSGA-II Algorithm to Multiobjective Reactive Power Planning, Applied Soft Computing, vol. 12, pp. 741–753, 2012.
35. J. Wiik, J O. Gjerde, T. Gjengedal, Steady State Power System Issues When Planning Large Wind Farms," IEEE Power Engin Soci Win Meeting, 2002, pp. 657–661.
36. Z. Xiang Jun, T. Jin, Z. Ping, P. Hui, W. Yuan Yuan, Reactive Power Optimization of Wind Farm based on Improved Genetic Algorithm, Energy Procedia, vol. 14, pp. 1362–1367, 2012.
37. A. Rabiee, M. Vanouni, M. Parniani, Optimal Reactive Power Dispatch for Improving Voltage Stability Margin Using a Local Voltage Stability Index, Energy Conversion and Management, vol. 59, pp. 66–73, 2012.
38. A. Ghasemi, H. Afaghzadeh, O. Abedinia, S.N. Mohammad, Artificial Bee Colony Algorithm Technique for Economic Load Dispatch Problem, Proceedings of EnCon2011 4th Engineering Conference Kuching, Sarawak, Malaysia, pp. 1–6, 2011.
39. Y. Wang, F. Li, Q. Wan, H. Chen, Reactive Power Planning Based on Fuzzy Clustering, Gray Code, and Simulated Annealing, IEEE Transactions on Power Systems, vol. 26, no. 4, pp. 2246–2255, 2011.